CHEMISTRY OF MATERIALS
Article

Chem. Mater. **2010,** *22,* 207–211 207
DOI:10.1021/cm902907e

Enhanced Performance of Dye-Sensitized TiO_2 Solar Cells Incorporating COOH-Functionalized Si Nanoparticles

Youngsoo Kim,[†] Chang-Ho Kim,[†] Yeonhee Lee,[‡] and Kang-Jin Kim*,[†]

[†]*Department of Chemistry, Korea University, Seoul 136-713, Republic of Korea and* [‡]*Chemical Analysis Center, Korea Institute of Science and Technology, Seoul 136-791, Republic of Korea*

Received September 17, 2009. Revised Manuscript Received November 12, 2009

Dye-sensitized solar cells (DSSCs) treated with COOH-functionalized Si (Si-COOH) nanoparticles exhibited a higher short-circuit photocurrent density (J_{sc}) and open-circuit voltage than the corresponding untreated DSSC. The enhanced J_{sc} is attributed to the sensitization resulting indirectly from the N719 dye attached to the Si-COOH nanoparticles by intramolecular charge transfer and directly from the Si nanoparticles anchored onto the TiO_2 film. As a result of the improved performance, the overall energy conversion efficiency was increased by 17%, as compared to that for a reference cell without the Si-COOH nanoparticles at 100 mW cm^{-2}.

Introduction

The design of efficient dyes has led to the instigation of specific strategies focused on searching for new dyes to sensitize TiO_2 over the entire visible range and with increased molar absorption coefficients for enhanced solar light utilization. Alternatively, semiconductor nanoparticles with small band gaps can be incorporated into a dye-sensitized solar cell (DSSC) in order to increase its light conversion efficiency via the extension of the absorption to wavelengths longer than those typically utilized by Ru(II) dyes.[1,2] This is due to the control of the optical properties achieved by changing the size of the nanoparticles. Several nanoparticles, including InAs,[3] InP,[4] CdS,[5−9] CdSe,[10−15] PbS,[7,16,17] Ag_2S,[7] Sb_2S_3,[7] Bi_2S_3,[7,18] and CdTe,[15] have been examined as sensitizers, but their contribution to the overall energy conversion efficiency remains low.[5]

Si nanoparticles, which are still the most widely used material for photovoltaic applications, are a promising, alternative candidate low band gap semiconductor to enhance the overall energy conversion efficiency of DSSCs. A variety of preparation techniques has been developed for Si nanoparticles, including the ultrasonic dispersion of porous Si,[19−21] gas-phase decomposition of silanes,[22−24] and solution methods employing inverse micellar synthesis.[25−28] It is advantageous for solar cell applications that the conduction band of the Si nanoparticles be located at a slightly more negative potential compared to that of TiO_2. Bulk Si exhibits an indirect band gap of 1.1 eV, but it has been reported that the electronic transitions in Si nanoparticles with a diameter of less than a few nm have a direct-like character, and therefore, possess high extinction coefficients.[6,29,30]

*Corresponding author. Tel.: +82-2-3290-3127. Fax: +82-2-3290-3121. E-mail: kjkim@korea.ac.kr.

(1) Luque, A.; Martí, A.; Nozik, A. J. *MRS Bull.* **2007**, *32*, 236.
(2) Nozik, A. J. *Physica E* **2002**, *14*, 115.
(3) Yu, P.; Zhu, K.; Norman, A. G.; Ferrere, S.; Frank, A. J.; Nozik, A. J. *J. Phys. Chem. B* **2006**, *110*, 25451.
(4) Zaban, A.; Mićić, O. I.; Gregg, B. A.; Nozik, A. J. *Langmuir* **1998**, *14*, 3153.
(5) Lee, W.; Lee, J.; Lee, S.; Yi, W.; Han, S.-H.; Cho, B. W. *Appl. Phys. Lett*. **2008**, *92*, 153510.
(6) Chang, C.-H.; Lee, Y.-L. *Appl. Phys. Lett*. **2007**, *91*, 053503.
(7) Vogel, R.; Weller, H. *J. Phys. Chem*. **1994**, *98*, 3183.
(8) Peter, L. M.; Riley, D. J.; Tull, E. J.; Wijayantha, K. G. U. *Chem. Commun*. **2002**, 1030.
(9) Wijayantha, K. G. U.; Peter, L. M.; Otley, L. C. *Sol. Energy Mater. Sol. Cells* **2004**, *83*, 363.
(10) Kongkanand, A.; Tvrdy, K.; Takechi, K.; Kuno, M.; Kamat, P. V. *J. Am. Chem. Soc*. **2008**, *130*, 4007.
(11) Liu, D.; Kamat, P. V. *J. Phys. Chem*. **1993**, *97*, 10769.
(12) Fang, J.; Wu, J.; Lu, X.; Shen, Y.; Lu, Z. *Chem. Phys. Lett*. **1997**, *270*, 145.
(13) Robel, I.; Subramanian, V.; Kuno, M.; Kamat, P. V. *J. Am. Chem. Soc*. **2006**, *128*, 2385.
(14) Robel, I.; Kuno, M.; Kamat, P. V. *J. Am. Chem. Soc*. **2007**, *129*, 4136.
(15) Lee, H. J.; Kim, D.-Y.; Bang, J.-S.; Kim, S.; Park, S.-M. *Bull. Korean Chem. Soc*. **2007**, *28*, 1.
(16) Plass, R.; Pelet, S.; Krueger, J.; Gräzel, M. *J. Phys. Chem. B* **2002**, *106*, 7578.
(17) Hoyer, P.; Könenkamp, R. *Appl. Phys. Lett*. **1995**, *66*, 34.
(18) Peter, L. M.; Wijayantha, K. G. U.; Riley, D. J.; Waggett, J. P. *J. Phys. Chem. B* **2003**, *107*, 8378.
(19) Heinrich, J. L.; Curtis, C. L.; Credo, G. M.; Kavanagh, K. L.; Sailor, M. J. *Science* **1992**, *255*, 66.
(20) Bley, R. A.; Kauzlarich, S. M.; Lee, H. W. H.; Davis, J. E. *Mater. Res. Soc. Symp. Proc*. **1994**, *351*, 275.
(21) Bley, R. A.; Kauzlarich, S. M.; Davis, J. E.; Lee, H. W. H. *Chem. Mater*. **1996**, *8*, 1881.
(22) Brus, L. E.; Szajowski, P. F.; Wilson, W. L.; Harris, T. D.; Schuppler, S.; Citrin, P. H. *J. Am. Chem. Soc*. **1995**, *117*, 2915.
(23) Fojtik, A.; Weller, H.; Fiechter, S.; Henglein, A. *Chem. Phys. Lett*. **1987**, *134*, 477.
(24) Littau, K. A.; Szajowski, P. J.; Muller, A. J.; Kortan, A. R.; Brus, L. E. *J. Phys. Chem*. **1993**, *97*, 1224.
(25) Heath, J. R. *Science* **1992**, *258*, 1131.
(26) Bley, R. A.; Kauzlarich, S. M. *J. Am. Chem. Soc*. **1996**, *118*, 12461.
(27) Bley, R. A.; Kauzlarich, S. M. *Synthesis of Silicon Nanoclusters*; Fendler, J. H., Ed.; Wiley-VCH: Weinheim, Germany, 1998; pp 101−118.
(28) Bley, R. A.; Kauzlarich, S. M. *A New Solution Phase Synthesis for Silicon Nanoclusters*; Kluwer Academic Press: Netherlands, 1996, pp 467−475.
(29) Rosso-Vasic, M.; Spruijt, E.; van Lagen, B.; De Cola, L.; Zuilhof, H. *Small* **2008**, *4*, 1835.
(30) Holmes, J. D.; Ziegler, K. J.; Doty, R. C.; Pell, L. E.; Johnston, K. P.; Korgel, B. A. *J. Am. Chem. Soc*. **2001**, *123*, 3743.

Published on Web 12/02/2009

The band gap of Si nanoparticles varies from 1.1 to 5.4 eV depending on their sizes.[31] The relationship between the band gap and size of the Si nanoparticles can be fitted experimentally as $E(\text{eV}) = 1.13 + 13.9/d^2$, where d is the diameter of the Si nanoparticles in nm.[32] This suggests that Si nanoparticles with a size of 5-nm, for example, should be able to inject electrons into the conduction band of TiO_2 upon the absorption of solar light shorter than 735 nm when they are anchored onto the TiO_2 film. The incorporation of Si nanoparticles into conventional DSSCs can thus extend the sensitization of TiO_2 beyond the wavelengths harvested by the usual Ru(II)-bipyridyl complexes such as N719 dye. Moreover, Si can form strong and stable covalent bonds with organic materials, thus facilitating the possible linking of the Si nanoparticles to the TiO_2 film. Many routes have been developed for preparing organically functionalized Si nanoparticles. To enable the linking of Si nanoparticles to TiO_2 possible, they should be functionalized with appropriate groups such as COOH, NH_2, or phosphonate.[33,34]

In this study, we utilize the inverse micellar synthesis method[35] to produce Si nanoparticles, functionalize them with 4-vinylbenzoic acid, and study their influence on the performance of the DSSCs. 4-Vinylbenzoic acid was selected here instead of the commonly used acrylic acid[33,36] in order to avoid possible steric hindrances between Si nanoparticles and TiO_2 particles. We first discuss the characterization of the COOH functionalized Si (Si-COOH) nanoparticles. We then present the enhanced photocurrent of DSSCs having a TiO_2 film treated with Si-COOH nanoparticles with the goal of increasing the effective sensitizer concentration of the film. To the best of our knowledge, this is the first report on the effects of the treatment of TiO_2 films with Si nanoparticles on the performance of the resulting DSSCs.

Experimental Section

For the preparation of the Si nanoparticles,[37] 0.0918 mL of $SiCl_4$ was dissolved in 100 mL of dehydrated toluene containing 1.5 g of tetraoctylammonium bromide (TOAB). To this solution, a 2-fold excess of 1.0 M $LiAlH_4$ in THF was added to form the Si nanoparticles. The solution was left to react for 3 h, after which 20.0 mL of dehydrated methanol was slowly added to quench the remaining reducing agent. At that point, the surface of the Si nanoparticles was terminated with hydrogen.[31,38] The nanoparticles were then capped with carboxylic acid groups using 2.0 mL of 0.1 M 4-vinylbenzoic acid in methanol with 100 μL of 0.05 M H_2PtCl_6 in isopropyl alcohol as a catalyst

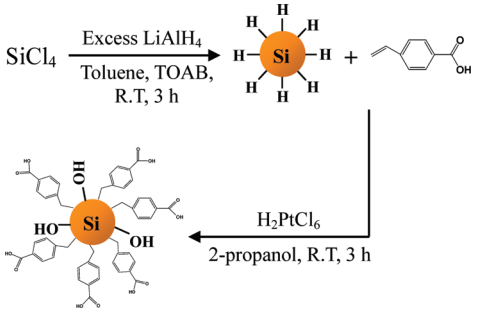

Figure 1. Schematic representation of the preparation of the COOH-functionalized Si (Si-COOH) nanoparticles.

(Figure 1). After 3 h,[39] the solvent was removed under vacuum to obtain a white powder consisting mainly of TOAB and the modified Si nanoparticles. To the powder, 50.0 mL of distilled water was added and the nonsoluble TOAB was filtered off. Finally, the water was removed by a vacuum evaporator to obtain the Si-COOH nanoparticles which were then dissolved in ethanol.

A thin layer of nonporous TiO_2 was deposited on cleaned FTO glass (Libbey-Owens-Ford TEC 8), using 5% titanium(IV) butoxide in ethanol by spin coating at 3000 rpm followed by annealing at 450 °C. The TiO_2 film was then obtained by spreading titania paste (Dyesol Ltd.) on the conducting glass substrate using a doctor blade technique, followed by annealing at 450 °C. The resulting TiO_2 film was first coated with the Si-COOH nanoparticles in ethanol solution. The Si-COOH treated TiO_2 film (Si-COOH/TiO_2) was then sensitized with the dye by immersing it for 24 h in a 0.3 mM ethanol solution of the N719 dye ($Ru(II)L_2(NCS)_2$:2TBA, where L = 2,2′-bipyridyl-4,4′-dicarboxylic acid, Solaronix SA). A 2-electrode sandwiched DSSC was fabricated according to a previously reported procedure[40] with an active area of 0.4 cm × 0.4 cm. A thin TiO_2 film with a thickness of 10 μm was used unless otherwise specified. The electrolyte consisted of 0.05 M I_2, 0.1 M LiI, 0.6 M 1-hexyl-2,3-dimethylimidazolium iodide, and 0.5 M 4-*tert*-butylpyridine in 3-methoxypropionitrile. Another DSSC was prepared as a reference cell under identical conditions, but without using Si-COOH nanoparticles.

The $J-V$ measurements of the DSSCs were carried out with a Keithley 2400 source-measure unit under AM 1.5 conditions, using a 1000 W xenon lamp with a KG-5 filter. The light intensity was adjusted to 100 mW cm^{-2} using a Si solar cell. The IPCE spectra were measured using a photon counting spectrofluorimeter (ISS PCI) equipped with a 350 W Xe lamp and a motorized monochromator. The Si nanoparticles were characterized by HR-TEM (FEI Co., Technai F20), UV−vis absorption spectroscopy (HP 8453A), and FT-IR spectroscopy (Perkin-Elmer, Spectrum GX). The elemental analysis of Si was conducted by ICP-AES (Varian, 710-ES).

Results and Discussion

Characterization of Si-COOH. HR-TEM was used to characterize the Si-COOH nanoparticles. Figures 2a and 2b show the HR-TEM images of a number of the Si-COOH nanoparticles on an amorphous carbon coated-copper grid. The figures display the formation of spherical Si particles with sizes ranging from 2 to 10 nm. Contrary to the expectation, however, the fast Fourier

(31) Wilcoxon, J. P.; Samara, G. A. *Appl. Phys. Lett.* **1999**, *74*, 3164.
(32) Kim, T. -W.; Cho, C. -H.; Kim, B. -H.; Park, S.-J. *Appl. Phys. Lett.* **2006**, *88*, 123102.
(33) Rogozhina, E. V.; Eckhoff, D. A.; Gratton, E.; Braun, P. V. *J. Mater. Chem.* **2006**, *16*, 1421.
(34) Warner, J. H.; Hoshino, A.; Yamamoto, K.; Tilley, R. D. *Angew. Chem., Int. Ed.* **2005**, *44*, 4550.
(35) Tilley, R. D.; Yamamoto, K. *Adv. Mater.* **2006**, *18*, 2053.
(36) Sato, S.; Swihart, M. T. *Chem. Mater.* **2006**, *18*, 4083.
(37) Baldwin, R. K.; Pettigrew, K. A.; Ratai, E.; Augustine, M. P.; Kauzlarich, S. M. *Chem. Commun.* **2002**, 1822.
(38) Wilcoxon, J. P.; Provencio, P. P.; Samara, G. A. *Phys. Rev. B: Condens. Matter. Phys.* **1999**, *60*, 2704.
(39) Tilley, R. D.; Warner, J. H.; Yamamoto, K.; Matsui, I.; Fujimori, H. *Chem. Commun.* **2005**, 1833.
(40) Kang, M. G.; Park, N.-G.; Chang, S. H.; Choi, S. H.; Kim, K.-J. *Bull. Korean Chem. Soc.* **2002**, *23*, 140.

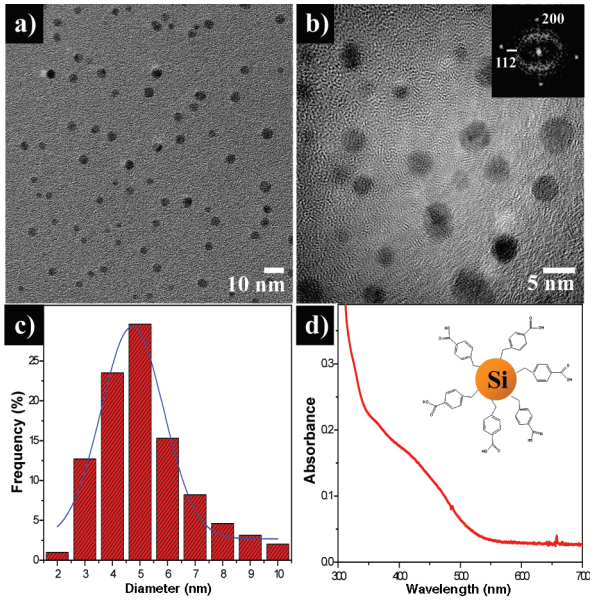

Figure 2. (a,b) HR-TEM images of the Si-COOH nanoparticles. The inset in (b) shows the typical FFT electron diffraction pattern corresponding to one of the nanoparticles. (c) Size distribution of 196 randomly selected the Si nanoparticles. (d) UV−vis absorption spectrum of the Si nanoparticles in ethanol.

transform electron diffraction (FFT-ED) pattern displayed in the inset of Figure 2b is found to correspond closely to the (200) and (112) planes of the hexagonal SiO_2 with the reference data (JCPDS card 87−2096). The (200) and (112) planes are separated by a distance of d = 2.12 and 1.83 Å, respectively. This result was attributed to the partial oxidation of the Si-COOH nanoparticles and their capping with the organic material. The surface of the nanoparticles was partially oxidized, despite their fabrication in an N_2 atmosphere to prevent their oxidation. The size distribution (Figure 2c) determined from 196 randomly chosen nanoparticles from different regions of the TEM grid yielded an average size and standard deviation of 4.7 ± 1.1 nm. Figure 2d presents a typical absorption spectrum of the Si nanoparticles in ethanol over the wavelength range of 340 - 550 nm. It shows that the band edge (~1.7 eV) corresponding to the onset at 750 nm is blue-shifted in comparison with that (1.1 eV) of the bulk Si. This is consistent with the recent study in which the band gap energy was calculated to be 1.76 eV from the relationship, $E_g(\text{eV}) = 1.13 + 13.9/d^2$, for a d value of 4.7 nm.[32] The broad nature of the spectrum indicates the growth of the Si nanoparticles with a wide particle-size distribution in the reaction process, which is consistent with the HR-TEM data (Figure 2c).

The bonding of 4-vinylbenzoic acid to the Si nanoparticles was identified in the FT-IR spectrum (Figure 3) with the appearance of a C=O stretching band at 1630−1680 cm^{-1} and Si-CH_2 rocking band around 1470 cm^{-1}, and the disappearance of the =C−H rocking band near 1300 cm^{-1} and $=CH_2$ wagging band near 950 cm^{-1} of 4-vinylbenzoic acid.[36] The appearance of the peak between 1000−1100 cm^{-1}, attributable to the vibrational stretching of Si-OR,[36] suggests that the surface of the Si nanoparticles is partially oxidized, which is consistent with the inset in the HR-TEM image in Figure 2b.

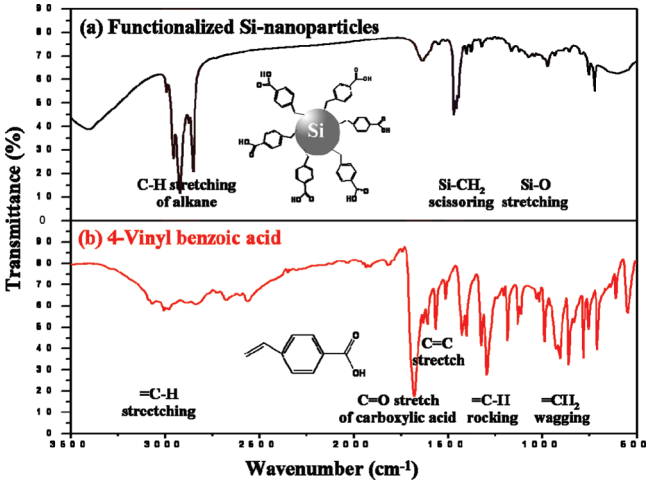

Figure 3. FT-IR spectra of (a) the Si-COOH nanoparticles and (b) 4-vinylbenzoic acid.

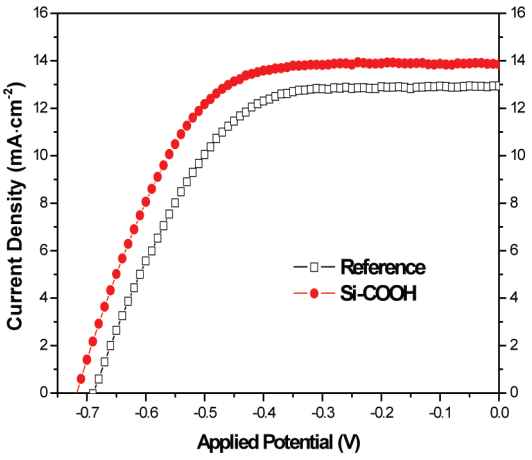

Figure 4. $J-V$ curves of DSSCs consisting of TiO_2 films treated (solid circles) and untreated (open squares) with the Si-COOH nanoparticles. Film thickness: 10 μm. Light intensity: 100 mW cm^{-2}.

Table 1. Photovoltaic Parameters of DSSCs Treated and Untreated with the Si-COOH Nanoparticles at Two Different TiO_2 Film Thicknesses[a]

thickness (μm)	Si-COOH	J_{sc} (mA cm^{-2})	V_{oc} (V)	FF (%)	η (%)
4 ± 0.4	without	7.97 ± 0.22	0.67 ± 0.01	67 ± 3	3.6 ± 0.2
	with	8.82 ± 0.22	0.70 ± 0.01	72 ± 3	4.4 ± 0.2
10 ± 0.4	without	12.9 ± 0.22	0.69 ± 0.01	58 ± 3	5.2 ± 0.2
	with	13.8 ± 0.22	0.71 ± 0.01	61 ± 3	6.1 ± 0.2

[a] Average of three measurements. Uncertainties are ± one standard deviation.

***J−V* Characteristics.** The influence of the TiO_2 film incorporating the Si-COOH nanoparticles deposited from an ethanol solution on the performance of the DSSCs was evaluated. Two different TiO_2 film thicknesses were used: 4 and 10 μm. The resulting $J-V$ curves of the DSSCs treated and untreated with the Si-COOH nanoparticles, at a light intensity of 100 mW cm^{-2}, are presented in Figure 4, and the corresponding photovoltaic characteristics are summarized in Table 1. Although the amount of elemental Si relative to the amount of TiO_2 in the treated film was measured to be 1.1% by elemental analysis, the J_{sc} (13.8 mA cm^{-2}), V_{oc} (0.71 V), and fill

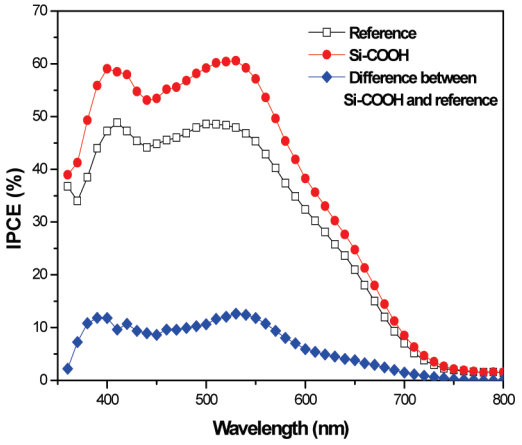

Figure 5. IPCE spectra of DSSCs treated (solid circles) and untreated (open squares) with the Si-COOH nanoparticles and the difference spectrum (solid diamonds) between the two spectra.

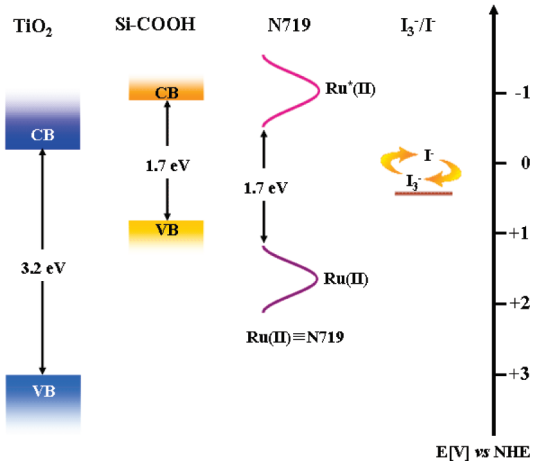

Figure 6. Energy diagram for TiO_2, the Si-COOH nanoparticles, N719, and the I_3^-/I^- couple.

factor (FF, 61%) values of the DSSC with the Si-COOH nanoparticles and the 10 μm-thick TiO_2 film are remarkably increased compared to the those of the reference cell, viz. 12.9 mA cm^{-2}, 0.69 V, and 58%, respectively. Promoted by these changes, the DSSC treated with the Si-COOH nanoparticles showed an overall energy conversion efficiency (η) of 6.1%, compared to 5.2% for the reference cell.

Table 1 also shows that the $J-V$ characteristics varied conspicuously with the thickness of the TiO_2 film. As the film thickness of the TiO_2 film increased from 4 to 10 μm, the J_{sc} value increased by 60%, irrespective of the modification with the Si-COOH nanoparticles, while the V_{oc} remained nearly the same, and the FF values decreased. Apparently, the thicker TiO_2 film lost disproportionally more electrons than the thinner one, possibly by recombination. The FF value decreased with increasing TiO_2 film thickness, because of the increased resistance.

Enhanced J_{sc}. The 7% increase (0.9 mA cm^{-2}) in the J_{sc} value observed in the treated DSSC relative to that of the untreated cell (Table 1) was supported by the IPCE spectrum shown in Figure 5. The IPCE values were increased over the entire visible range by the treatment. Furthermore, the difference in the IPCE spectrum, indicated in the figure by diamond symbols, obtained by subtracting the IPCE values of the treated cell from those of the untreated cell, is qualitatively in good agreement with the absorption spectrum of the N719 adsorbed on the TiO_2 film. From these results, the J_{sc} increase was attributed primarily to the enhanced adsorption of N719.

The Si-COOH nanoparticles clearly influenced the photocurrent increase. The J_{sc} increase was considered attributable to both the direct sensitization induced by the Si-COOH nanoparticles and the indirect sensitization induced by the N719 molecules anchored to the Si-COOH nanoparticles, based on the following observations. First of all, in the blank test without using N719, the photocurrent of the DSSC with the Si-COOH/TiO_2 film was increased by 0.06 mA cm^{-2} relative to that of the cell without the Si-COOH nanoparticles, which was clearly attributed to the direct sensitization of the TiO_2 film by the Si-COOH nanoparticles. As shown in Figure 6 and based on the results shown in Figure 4, the Si-COOH nanoparticles, in a similar manner to N719, appear to have formed favorable energy relationships both with the conduction band edge of TiO_2 for electron injection and with the valence band of the Si nanoparticles for the regeneration of holes by the iodide in the electrolyte, leading to the generation of a photocurrent according to eq 1

$$Si(h^+) + I^- = Si + 1/2I_2 \qquad (1)$$

However, the direct sensitization contributed only slightly to the J_{sc} increase. The reasons could be that only a small quantity of the Si-COOH nanoparticles was incorporated into the TiO_2 film, as shown above, and that some of them was expected to emit photoluminescence upon excitation, possibly because the Si-COOH nanoparticles were linked to the TiO_2 particles through the rather long, $-(CH_2)_2-C_6H_4-COO^-$ linkage. The emission of the blue photoluminescence was confirmed from the ethanol solution of the Si-COOH nanoparticles by the light of 355 nm. The degree of the direct sensitization was clearly insufficient to explain the 0.9 mA cm^{-2} increase in the J_{sc}. To explain this discrepancy, we measured the amount of dye adsorbed onto the Si-COOH/TiO_2 film. This was evaluated by measuring the absorbance of dye desorbed from the TiO_2 film into 10 mM KOH solution by UV−vis spectroscopy. The results shown in Figure 7a indeed indicated that 7% more N719 was adsorbed onto the Si-COOH/TiO_2 film than onto the reference TiO_2 film. In addition, the absorbance of the dye-adsorbed TiO_2 film was monitored. Figure 7b reveals that N719 adsorbed 7% more onto the Si-COOH/TiO_2 film than on the reference TiO_2 film. The absorption spectrum is slightly red-shifted, indicating the adsorption of N719. These results clearly suggested that the N719 molecules were also attached to the Si-COOH nanoparticles, because the effective surface area for the adsorption of N719 onto the TiO_2 film was decreased after the anchoring of the Si-COOH nanoparticles onto the TiO_2 surface. The attachment of N719 to the Si-COOH nanoparticles was qualitatively confirmed by the persistent appearance of its characteristic color to the naked eye, upon immersing a

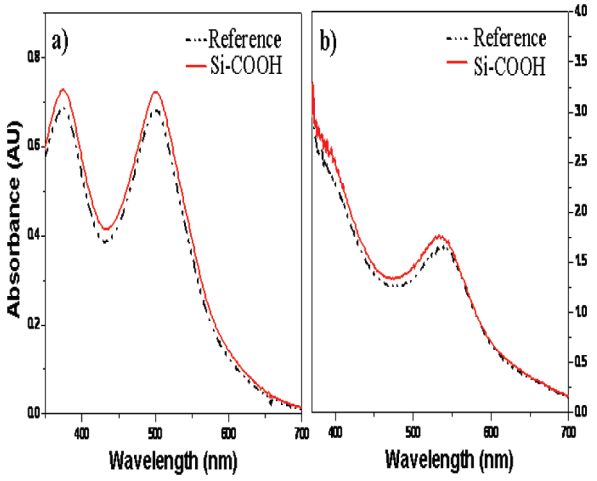

Figure 7. UV−vis absorption spectra of N719 (a) desorbed from TiO_2 film into KOH solution and (b) anchored on the TiO_2 film.

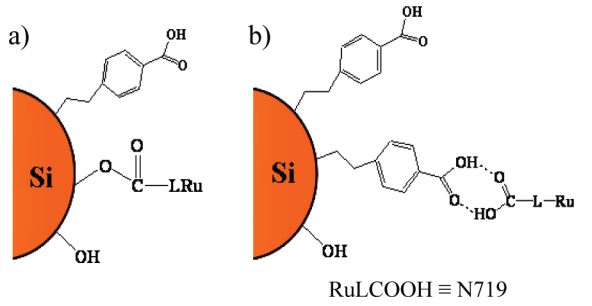

Figure 8. Postulated mechanism for the increased amount of dye adsorption by (a) attachment of dye onto the hydroxylated Si nanoparticle and (b) formation of the carboxylic acid dimer.

Si-COOH coated FTO glass into the ethanol solution of N719.

Two possible mechanisms exist to explain the attachment of N719. First, the dye molecules may be attached to the hydroxylated surface of the Si-COOH nanoparticles, similarly to the way in which N719 is anchored to TiO_2, as illustrated in Figure 8a. The presence of Si−OH on the Si-COOH nanoparticles is inevitable, because the Si nanoparticles are exposed to air during the synthetic process. The second possibility is through the formation of the dimerlike structure shown in Figure 8b. To explain the J_{sc} increase, it is hypothesized that the N719, upon excitation, is able to transfer electrons to the conduction band of TiO_2 through the Si-COOH nanoparticles to which it is attached. This hypothesis was supported by the recent reports in which the enhancement of the J_{sc} value was attributed to the efficient intramolecular charge transfer from the linked dye molecules to the immobilized dye molecules through a chain of conjugated double bonds.[41,42]

The next question arising is the extent of the contribution of the increased amount of N719 to the J_{sc} enhancement. The J_{sc} increase may be entirely due to the increased amount of N719 adsorbed onto the Si-COOH/TiO_2 film, base on the identical 7% increases in the J_{sc} and in the adsorbed dye relative to those obtained for the untreated cell. However, the observed J_{sc} value was smaller than that expected because the dye molecules whose energy levels lie above the conduction level of the Si nanoparticles can inject electrons into the conduction band of TiO_2, as can be judged from Figure 6.[43] As a result, not all of the dye molecules attached to the Si-COOH nanoparticles contribute indirectly to the J_{sc} increase. Therefore, we conclude that both the indirect and direct sensitizations contribute to the J_{sc} increase.

Enhanced V_{oc}. The enhanced V_{oc} value of the DSSC with the Si-COOH nanoparticles shown in Figure 4 may be explained in terms of the decreased back electron transfer from the TiO_2 conduction band to the I_3^- ions in the electrolyte. The Si-COOH nanoparticles on the TiO_2 film, as well as those on the TiO_2/FTO glass interface, reduce the contact between the electrode and electrolytic solution, thereby decreasing the rate of back electron transfer compared to that in the absence of the nanoparticles.[44] The V_{oc} increase decreased the J_{sc} value, because the electron injection from the excited N719 molecules anchored on the TiO_2 film decreases, due to the increased barrier height created by the enhanced V_{oc} value of the DSSC with the Si-COOH nanoparticles, compared to that in the reference cell.[41]

The primary focus of our research was to study the increase in the photocurrent due to the cosensitization by the Si-COOH nanoparticles anchored on the TiO_2 film and the charge transfer from the excited N719 molecules attached to them. Further research using a large number of size-optimized Si nanoparticles will be necessary to improve the overall energy conversion efficiency of the resulting DSSC.

Conclusions

We fabricated improved DSSCs by a novel approach based on the incorporation of Si-COOH nanoparticles into a TiO_2 film. Si nanoparticles with a size range of 2−10 nm were prepared by reducing $SiCl_4$ with $LiAlH_4$ in the presence of tetraoctylammonium bromide and subsequently reacting with 4-vinylbenzoic acid to produce the Si-COOH nanoparticles. The 10-μm thick TiO_2 film treated with the Si-COOH nanoparticles was employed for the first time to fabricate a DSSC with an overall energy conversion efficiency η of 6.1%, compared to 5.2% for the reference cell without the Si-COOH nanoparticles at an illumination intensity of 100 mW cm^{-2}. This increased conversion efficiency was attributed to the cosensitization by the Si-COOH nanoparticles and the charge transfer from the excited N719 molecules attached to the Si-COOH nanoparticles.

Acknowledgment. This work was supported by the KOSEF basic research project under contract 2009-0073457.

(41) Lee, Y.; Jang, S. -R.; Vittal, R.; Kim, K.-J. *New J. Chem.* **2007**, *31*, 2120.
(42) Jang, S.-R.; Vittal, R.; Lee, J.; Jeong, N.; Kim, K.-J. *Chem. Commun.* **2006**, 103.
(43) Park, N.-G.; Chang, S. -H.; van de Lagemaat, J.; Kim, K. -J.; Frank, A. J. *Bull. Korean Chem. Soc.* **2000**, *21*, 985.
(44) Lagref, J. -J.; Nazeeruddin, Md. K.; Gräzel, M. *Synth. Met.* **2003**, *138*, 333.